Review: The Application of Imaging Techniques SAFT As An Ultrasonic Monitoring System Support

Noor Amizan Abd. Rahman[1], Ruzairi Abdul Rahim[2*], Jaysuman Pusppanathan[3], Jamil Abedalrahim Jamil Alsayaydeh[4]

[1]School of Electrial Engineering, Faculty of Engineering,

Universiti Teknologi Malaysia, Skudai 81300, Johor, Malaysia

[2]Process Tomography Research Group, School of Electrical Engineering, Faculty Engineering, Universiti Teknologi Malaysia, 81310 UTM, Malaysia.
[3]Sports Innovation & Technology Centre (SiTC), Institute of Human Centered Engineering (iHumen), Faculty of Engineering, Universiti Teknologi Malaysia 81310 Skudai Johor.
[4]Center for Advanced Computing Technology, Fakulti Teknologi Kejuruteraan Elektrik dan Elektronik (FTKEE), UTeM, Hang Tuah Jaya, Melaka, Malaysia.

Corresponding author email: ruzairi@utm.my

Abstract

Monitoring the progress of the construction industry is recognized as one of the key elements to the success of a construction project. The implementation of these as corrective measures and other appropriate actions can be taken in a timely manner, thus enabling the actual performance to be as close as possible to the desired outcome. However, the methods used for data acquisition and their use in construction require more realistic image assistance in detecting defects. Applications and research on the rapidly expanding Synthetic Aperture Focusing Technique (SAFT), particularly in the field of disability monitoring involving the industrial and medical sectors. Ultrasonic Tomography (UT) monitoring method with SAFT imaging process as an advantage. The tendency for discussion on the development and construction of SAFT-UT images from signals received from senders and receivers used in the industry.

Keywords: Ultrasonic Tomography, Syenthetic Aperture Focusing Technique, Image Recontruction.

1. Introduction

Ultrasonic (UT) testing was first started in 1929 by the Sokolov Federation [1] using ultrasound for cast iron testing. Whereas in 1949 the commercial use of the Krautkrämer design was a market leader in the early 60s. In addition to Krautkramer Karl Deutsch and Nukem in Germany, Panametrics and Stavely in the US, Sonatest and Sonomatic in GB, Gilardoni in Italy and

Mitsubishi in Japan. From the 1980s to the present, computerized UT systems can be programmed for use in large materials / structure inspections, more complex components, systems using either single or multiple transducers [2]. Many researchers have proposed the use of Wiener filters [3] but the Synthetic Aperture Focusing Technique (SAFT) approach [4], is an option for flexible imaging that can be adapted to a wide variety of materials, specimen geometry, and ultrasonic propagation modes

Non-destructive testing (NDT) utilized non-invasive methods to assess the integrity of a material without changing the physical or chemical properties of the object. Ultrasonic testing is a non-destructive technique and it can be used to determine the defects in a material and can be used to determine the thickness of the sheets of blocks used in the industry [3]. Ultrasonic methods do not pose any hazard and are safe to use. It also does not damage the object to be investigated and does not harm anyone who conducts the investigation. Ultrasound has been used to characterize and detect defects [4]. An ultrasonic sensing system can transmit the required energy into and out of the wood. As an example, Brenjaux et al [5] investigates the use of high power ultrasound for oak wood barrel. Skowroński and Stawiski [6] conduct an investigation regarding the impact of corrosion on roof trusses using ultrasound.

Early applications of ultrasound monitoring from Prine's radar experience, 1972. Ultrasonic data were recorded on a photographic film using a phase reference or coherent decoder. The received signal is amplified by incorporating the reference source signal to give the coherent signal unscheduled on the oscilloscope. The oscilloscope output was recorded on a film using a camera scanned in synchrony with an ultrasonic transducer scan.

Improvements to recover ultrasound images obtained from B or C scans with a focus on recovery from distorted signals. This method is to increase the image resolution and maintain signal beam changes. This synthetic focus is based on the reflection or acoustic ray of the geometric model. The focus of the ultrasonic transducer is the continuous phase point of the sound wave passing through the source of the defect before deviating in the angular beam focus as determined by the transducer diameter and focal length [5].

2. Saft Fundermental

SAFT is a process of focusing openings on transducer signal widths such as the role of lenses during the imaging process series. The combination of control over the opening of the illumination is based on the choice of level for a more effective image [6]. Basic system parameters such as resolution, frame rate, and image uniformity show how resolution can be improved by receiving synthetic aperture, image uniformity with synthetic aperture transmitter with virtual sources, and synthetic frame rate [7].

The SAFT algorithm of the time domain [8] focuses on coherent aggregation at locations along the hyperbola in the region (ROI) in a gradual way to aperture on a focused image. This hyperbole simply represents the distance, or time delay of the transducer to the target position when the transducer is scanned in linear [9].

In practical implementation of SAFT imaging there is a balance between the size of the transducer and the need for signal to noise ratio (SNR) in the received signal. Using larger transducers can increase the SNR rate but at the same time the processing time [10] to identify the wave incompatibility of the transducer element reduces the quality of the reconstructed image. SAFT processing is a focal simulation for transducers [11], which is done in computer software. Some studies use the basic SAFT equation as follows:

$$I[x,y,z] = \frac{1}{N}\sum_{n=1}^{N} X_n[\frac{2r_n}{c}]$$

where N = is the number of transducers, Xn = represents the signal received by the transducer n, c = is the speed of sound in the media, rn = is the distance between the transmitter and transducer n [4].

The above equation uses high frequency wave support. However, at the beginning of the study it was not suitable for monitoring of elements of wood and concrete and usually only used very low frequencies (about 100 kHz).

According to a previous study the diameter of the transducer affects the resolution level [12], for example if large size interferes with the intensity of the image resolution [13]. Image defects are first detected by ultrasound reflection waves. Data called echo pulse [14] is used to transmit and receive ultrasound data. Signal sources and receivers that produce high voltage pulses.

Pulses received in vibrating waves such as ultrasound waves [15], from defects received. At the same time the pulse is processed from analogue to digital (A / D) [16]. In general, the flow process is summarized as shown in Figure 1 below.

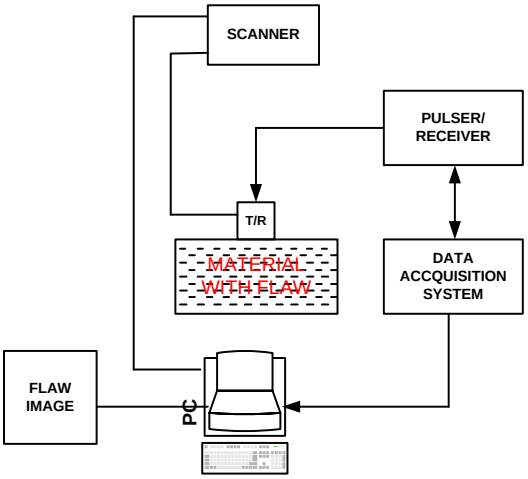

Figure 1 The process of ultrasonic flow monitoring system for the material flow.

3. Saft Fundermental

The transducer is used to transmit and receive ultrasonic waves [17] with the received signal as shown in Figure 2. The raw signal is received along with the noise. The signal processing method [18] uses filters to obtain clean signals.

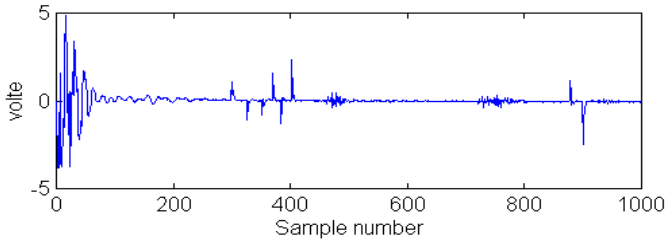

Figure 2 Example of raw signal received from transducer

At each point 256 times the data is collected and their average is considered acceptable [19] as shown in Figure 3. The signal marked "a" represents a reflection of the first contact area between the transducer and the material, "b" represents a reflection of the defect (s), "c" is a reflection of the back wall and "d" is a repetition of "b". The assumption of such a signal is repeated [20].

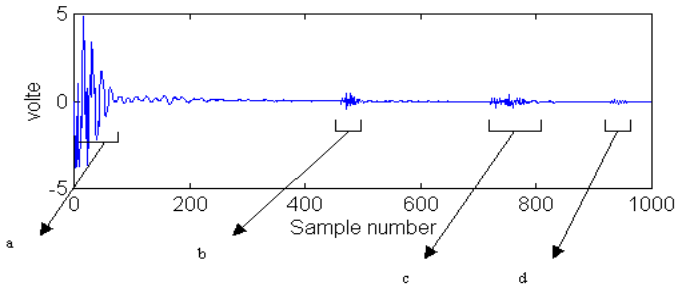

Figure 3 Classification of raw signals before processing

Signal frequency is 125 kHz with 75 kHz bandwidth [21]. Based on the sampling frequency, the analogue signal sampling frequency theorem [22] must be greater or twice the largest frequency in the signal [23]. It was found that the recorded data were time-dependent but using ultrasound velocities in time-averaged media could be translated between the two samples, there was a 1 / FS time difference in which FS was the sampling frequency. When the time axis is translated to the axis, between two samples there is a C distance / Fs [24]. This means that vertical resolution depends on the ultrasound speed and frequency of sampling. For certain materials the velocity cannot be changed. Therefore, higher resolution requires higher FS. Typical frequency band 2 MHz sampling is used [25].

SAFT can also be implemented in the frequency domain using Fourier transform [26]. It is the solution to the problem of scattered inverse signals. Furthermore, SAFT is a technique of computing space, which has several practical advantages. For example, it can reduce noise and blurred images by increasing the signal-to-noise ratio (SNR) [27]. If the target is located below the centre of focus and in the beam curve, it is easy to calculate the wavelength and transit signal time. Beam widths are conical curves at a given distance equal to the width of the synthetic aperture, and the signal must travel parallel to the phase displacement to be carried to the transducer position. This information makes it possible to build a corrected data set that incorporates the benefits of a larger aperture transducer.

Refer to Figure 4, X1 as the source of the signal wave. While X2 is considered a defect in the material. The image will look like Figure 5, where 'd' refers to the thickness of the material tested [28]. The width of the scan space depends on the opening width of the transducer signal used.

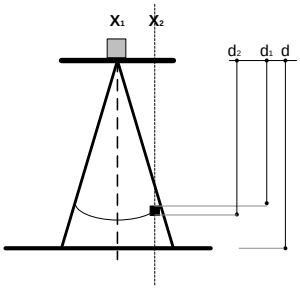

Figure 4 Transducer beam width on the test block, showing the inspection position X_1 and the defect position at X_2

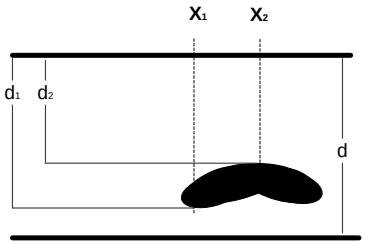

Figure 5 Distorted image resulting due to the beam width during a B-scan. The defect is at position (X_2, D_2)

The large image resulting from scanning is caused by the wide-open transducer [29], as shown in Figure 6. The algorithm selects and recalculates the points from the rows in the A-scan and subsequently associates these signals to enhance the obtained image.

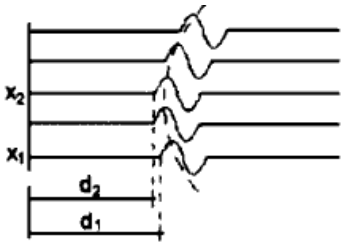

Figure 6 Schematics of A-scan signals which compose the B-scan image

4. Saft Fundermental

The aperture transducer cone is a model of geometric reflection [30]. This algorithm works for three dimensions but the previous study only used two dimensions. Referring to Figure 6, 'd2' is the distance the echo from the defect in X2 appears to X1. Thus the distance 'd2' can be calculated from the equation below:

$$d_3 = [\, d_2^2 + (x_1 - x_2)^2 \,]^{1/2} \quad \text{atau dalam bentuk lebih generic,} \qquad (2)$$

$$d_n = [\, d_A^2 + (x_A - x_n)^2 \,]^{1/2} \qquad (3)$$

Where xA = or x as the A-scan line, xn = A-scan line position near xA line, dn = the distance between the surface of the front block and the reflection of the pulse, dA = the distance from the material surface and the pulse of the system signal.

Figure 7a, 7b and 7c describe the correction process during the A-scan line transition that presents the echo signal due to defects in X2, together with the position of the two adjacent rows (four-line window), corrected in such a way that it appears that the defect started in X1. After this correction a correlation between the five rows is made which results in zero. Figure 7c illustrates the line in X2, which presents the position of the corrected signal for X2, and since the defect is as assumed in X2, the correlation between the five rows is now maximum.

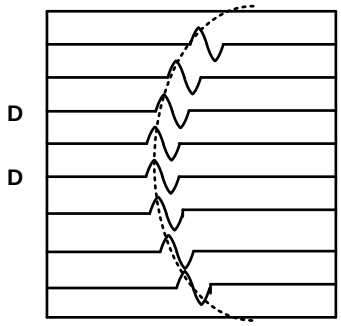

Figure 7a shows the A-scan sequence with the dashed line showing curvature due to the beam

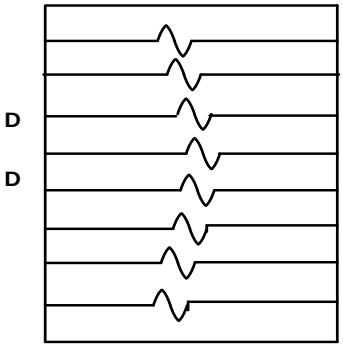

Figure 7b shows the SAFE process for the line in X1, which presents the echo signal due to a defect in X2 [4]

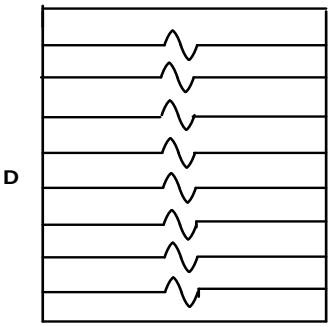

Figure 7c illustrates the actual process for the lines in X2 (real) corrected [4]

As we can see, the signal from the adjacent position (consisting of the aperture) is moving to the appropriate phase and added to the first signal. If that assumption is correct, the summary result is an enhanced response; if wrong, there is a weak or zero relationship. The implied correlation process in the window region adjacent to the correction line is made only after the correction procedure has been taken place. This correlation is obtained by summing the lines along the lines [4]:

$$x_r(k) = (1/m) \sum_{n=A-m/2}^{A+m/2} x_A(k)\, x_n(k)$$

If 'm' is the sum of the number of adjacent lines (correlation window widths), lines A, and 'k' represents the distance from the surface of the test material is generally different, the line resulting in Xr corrected 'k' is then calculated according to equation (4).

5. Previous Of SAFT Application

The SAFT process is particularly popular in studies of the detection of internal defects in thick steel plates, we employ synthetic aperture focusing technique (SAFT) to find and visualize internal defects of steel plates. The source of the moving pulse laser source is used to produce longitudinal ultrasonic waves in steel samples. Laser vibrations are used to obtain B-scan ultrasound domain signals at fixed points. Longitudinal echo waves are reflected by defects extracted from domain time signals. And the internal defect imaging of the sample was realized. This imaging process was simulated numerically by finite element method (FEM) and validated in experiments. Experiment results coincide with numerical calculation results. Defective imaging methods that realize the detection of defects under conditions were defective

echo waves have low signal-to-noise ratio (SNR). The process is simple and straightforward, and it has practical value in the field of laser-ultrasonic detection [31].

There are studies on the effects of acoustic nonlinearity (CAN) visualized by synthetic aperture focusing (SAFT) techniques through signal processing methods for acoustic nonlinear imaging. The proposed signal processing technique, called Synthetic Aperture Imaging of Nonlinearity Acoustic (SAIAN), enables SAFT to visualize CAN that is difficult to visualize by linear ultrasound imaging. Using the SAIAN algorithm, the basic and second harmonic frequency components are extracted from the burst tone wave signal and then the component signal is converted to pulse-like signal. To confirm the effectiveness of the SAIAN, non-linear ultrasound measurements using broken waveforms were performed to visualize the interface closure. As a result, the CAN effect appears on some of the interfaces in the CAN image of the CAN converter; In contrast, the CAN feature is not shown in the linear ultrasound image based on the fundamental frequency components. These results support that SAIAN is a useful signal processing for acoustic nonlinear visualization that increases the detection probability between closure and accuracy in crack measurements [32].

In ultrasonic non-destructive testing, when using ultrasonic linear array transducers for nonplanar surface imaging objects, coupling medium must be used. To balance the refinement of the interface of the coupler object, the shape must be known. Two methods for surface detection of convex objects in immersion are proposed, using the same linear array transducer for surface detection and for SAFT imaging. One is based on imaging techniques and the other is based on the time-of-flight from the echo on the captured ultrasound signal. The accuracy and performance of both methods is compared to an experiment with an existing fast method called pitch-catch. The proposed method produces smaller errors in some of the tested configurations, with slower performance than the capture method. After surface detection, in the phase of SAFT image formation, delays are calculated using the proposed technique and fast to determine the fastest path, according to Fermat's principle. Images are formed for nine different groups of elements, and then combined using an effective aperture technique. The results show that the method developed allows the creation of interactive two-medium images on general purpose CPUs [33].

Laser pulses illuminate the target zone which results in rapid therapeutic development, producing high-frequency ultrasound waves (photoacoustic waves, PA waves). We developed a PA (PAM) microscope with laser and ultrasound vision areas for applications in non-volatile (NDT) testing. Synthetic aperture focusing (SAFT) techniques are used in PAM for three-dimensional (3D) imaging of internal defects. Here, we report experimental evidence for the NDT of surface defects in thin laminated materials. Graphic graph (a) shows carbon fibre reinforced plastic (CFRP) specimens with artificial healing. Here, it should be noted that the velocity of the group varies sequentially due to the strong anisotropy of the CFRP specimen (see Abstract Graph (b)). Considering the velocity distribution of the groups in the SAFT, the shape and location of the underwater spraying are precisely estimated as shown in the Abstract graph (c). The surface coating of CFRP specimens with light-absorbing material increases the amplitude of the PA wave. These findings indicate that the signal-to-noise ratio of the scattered waves can be improved [34].

The reinforcement of steel reinforcement in concrete structures is one of the causes of structural deterioration in the form of concrete cover cracks that can lead to more moisture and damage the rebar. Early detection of cracks caused by corrosion using non-destructive techniques can be helpful in scheduling maintenance activities. In this paper, we present ultrasonic imaging techniques to evaluate changes in concrete surfaces, during various stages of rebar corrosion. Accelerated corrosion preparation was developed to induce corrosion in rebar embedded in concrete slab specimens; Field capture mode along with ultrasonic scanning is performed on a set of grid points on test specimens. A variant of Aperture Focus Technique (SAFT) is used to produce flat slab images through slabs at various depths. The limited directivity effect of transducers is included in the algorithm for image generation. Studies show that with corrosion advances, rebar signatures are missing from the SAFT image, which could be a useful diagnostic indicator for rebar corrosion. In structures that generate realistic corrosion, the proposed technique can provide useful input into the scheduling of further inspection, repair and maintenance activities [35].

The development of the current ultrasound pulse-echo system is supported by the increased reliability of the inspection results. The application of the Synthetic Aperture Focusing Technique (SAFT) is one of the solutions to this problem. Implementation of SAFT-based post processing algorithms is highly dependent on ultrasonic scanning conditions. In this paper,

issues related to the implementation of SAFT in the case of welding ultrasonic examination are considered. As a result, a post-processing algorithm, which takes into account the key features of the object's inspection, is proposed. The capabilities of the proposed algorithm have been verified through computer simulation. It has been determined that the proposed algorithm can give an accurate and accurate picture of the disadvantages of welding [36].

One of the UTs implemented for process forgings, usually one of the most critical components especially in power generating machines, requires intensive volumetric inspection to ensure adequate life. This is usually done by manual or automatic ultrasound testing. The author reports on game changers in ultrasound testing: Ultrasonic Computed Tomography uses analytical (that is, mathematical algorithms) to reconstruct the volume (It even uses a straightforward, straightforward tomography-based approach to solving inverse problems). This not only allows the exhibit to display spatially and accurately on the 3D volume, but also increases the signal to noise ratio significantly, allowing for greater sensitivity to the magnitude. This method is based on Aperture Focused Aperture Technique (SAFT). The software being applied is a new application of SAFT with strong focus on large-scale industrial applications: 2D complete as well as 3D reconstruction of ultrasound examination of rotating heavy players [37].

Detection of cracks in structures welded to different materials using guided waves has not been well developed. This paper examines the effect of material permeability on plate structure and excess plastic deformation, at welded spacing (FSW), on the behavior of guided wave propagation towards their application in welding evaluation. Measuring the dispersion, softening and velocity of guided wave groups as they propagate across different media, as well as determining the elastic properties of materials in welds will provide rich information on the behavior of ultrasonic waves. Three free friction friction defects were used in this study. The first specimen is of different aluminum / magnesium alloy welding material (AA6061-T6 / AZ31B), the second is of different aluminum alloy grade (AA6060 / AA7020-T651) and the third is of the same aluminum grade (AA7020-T651 / AA7020-T651). Elastic properties across all welds were extrapolated using nano induction techniques. Ultrasonic guided waves are excited and measured using a piezoelectric wafer and a laser Doppler vibrometer (LDV). In addition, sensor network design was performed on three specimens using piezoelectric transducers. Wave reflection, based on LDV results and information gathered from the sensor

network, was observed in the welding zone AA6061-T6 / AZ31B FSW, while no reflection was detected in the welding zone on the AA7020-T651 / AA7020-T651 and AA6060 / AA7020-T651 plates. . The results are attributed to the measurements obtained from the nano-indentation experiments, where sharp changes in the elastic properties of the base metal in the welded connection AA6061-T6 / AZ31B were detected, unlike the other two plates showing elastic properties of welding zones. The results show that the amount of scattering in the joint is a function of the direction of the wave propagation. It has been observed that the average reflected wave is generated when the wave passing AZ31B to the base metal AA6061-T6 is about 35% of the incident signal, but it decreases to 25% when the wave propagation direction is reversed. Characterizing ultrasonic waves in FSWs and incident behavior and reflected waves in welded zones will improve the technology used for the examination and monitoring of solid-welded joints [38].

Studies on the detection of defects in dense joints in the early phase of multi-pass arc welding will be invaluable in reducing costs and time in the need for recycling. As a non-contact method, laser-ultrasound (LUT) technique has the potential for automatic welding inspection, eventually online during manufacture. In this study, the tests were conducted using LUT combined with synthetic aperture focusing technique (SAFT) at 25 and 50 mm thick butt welded steel joints both complete and partially welded. EDM slits of height 2 or 3 mm were inserted at different depths in a multi-pass welding process to simulate joint defects. Scanning of the horizontal line to the weld is done by the discovery and detection of laser spots sprayed directly onto the surface of the weld bead. CCD line cameras are used to simultaneously obtain surface profiles for correction in SAFT processing. All artificial defects but also actual defects are visualized in the specimens of thick back welding, either completed or partially welded after certain passes. The results clearly indicate the potential of using LUT with SAFT for automatic inspection of arc welding or laser-arc welding during manufacture [39].

Concrete is a composite material consisting mainly of water, sand, aggregates, and cement. High-resolution properties of concrete for ultrasound lower the performance of ultrasound (UT) tests, especially when the target size is significantly smaller than the aggregate. Recent advancements in electronic devices and computing technology have made comparisons between overall method (TFM) and staged (PA) techniques. However, the question of a better approach to UTof concrete remains unresolved. Early studies found that synthetic PA images,

similar to those obtained by PA systems, and synthetic TFM images, similar to those obtained by TFM systems, were made for UT concrete. The quality of these images is compared to that produced by traditional B-scans and synthetic aperture focusing (SAFT) techniques. Comparing the cost, complexity, complexity and efficiency of this technique, the results show that modern techniques (TFMand PA) are always better than traditional methods (B-scan and SAFT) based on 100 kHz ultrasonic experiments with low-to-noise ratio (SNR). The SAFT method can only improve the quality of B-scan images. In addition, a moderate distance between the source and the receiver is suggested to detect shallow and small targets in the concrete to avoid scattering backwards. However, the PA technique has the advantage of detecting small targets at specific depths in concrete. On the other hand, when detecting large targets in concrete, the TFM performs better than the PA technique. The results show that both PA and TFM have their own merits and demerits. PA performs well in low SNR environments, and TFM performs well in high SNR conditions. In conclusion, to detect small targets at specific depths in concrete, PA techniques are recommended. Otherwise, to detect large targets in concrete, TFM is a better choice [40].

There are also studies using the Phased Array Ultrasonic Technique (PAUT) method that offer great advantages over conventional ultrasound (UT) techniques, especially focal beam, beam steering and electronic scanning capabilities. However, the obtained 2D images usually have low resolution in the direction perpendicular to the array element, which limits the quality of inspection of large components by mechanical scanning. A new approach to improve image quality by combining three ultrasound techniques: Phased Array with dynamic depth focusing on reception, Aperture Targeting Synthetic Technique (SAFT) and Imaging Coherence Phase (PCI). The imaging algorithm shows that the obtained image quality is comparable to that obtained with a variety of equivalent matrices, but uses conventional NDT arrays and tools, and is implemented in real time [41].

As we can see, the signal from the adjacent position (consisting of the aperture) is moving to the appropriate phase and added to the first signal. If that assumption is correct, the summary result is an enhanced response; if wrong, there is a weak or zero relationship. The implied correlation process in the window region adjacent to the correction line is made only after the correction procedure has been taken place. This correlation is obtained by summing the lines along the lines [4]:

6. Previous of SAFT Application

Significant changes to ensure the integrity of the newly constructed pipeline, the detachment detector require proven and qualified technology. There is a study of the concept of current inspections based on (a combination of) zone discrimination, ToFD and well-known sectoral scans, the limitations inherent in inspection philosophy can lead to uneconomical compromises to ensure pipeline integrity. Due to advances in computer technology (faster processing and greater storage capacity), the development of the 'IWEX' (Inverse Wave Field Extrapolation) based on FMC (Full Matrix Capture (FMC)), as ultrasound data imaging, with innovative inspection techniques more recently, signs in intersection welding are recorded in real time in 2D and 3D. The images reveal the presence of signs where orientation, position, height, etc. are displayed in real context behind the back and front walls and the geometry of reinforcement and root reinforcement. Identification and measurement of the pointer can be done accurately and clearly, leading to reduced repair rates. Since the image is independent of welded bevel design, standard sensitivity blocks can be used, where the preparation work and number of calibration blocks are significantly reduced. To benefit from the full potential of this new screening technology, recipients industry is needed. Therefore, the system is subject to extensive eligibility program under DNV OS F101-2013, as it is a basic requirement of some major Oil and Gas pipeline companies. In addition, owners and contractors of the channel (engineering companies) may have their own additional requirements. Once the DNV qualification program has been completed successfully, IWEX imaging technology has been used in conjunction with standard AUT inspections during the actual project qualification program, as a joint venture between the pipeline owners, an engineering and inspection company. Additional details and requirements for validating IWEX imaging technology during the program. The study was carried out in two phases: 1) Confirmation of results obtained during DNV qualification. This phase involves welding examination with superior defects according to project-specific procedures. Position, height and length are verified using macro restrictions. 2) Durability test to evaluate the robustness of the system under actual production conditions. This phase involves welding scanning at the base of the spool, performing 12 hours of transition for 3 weeks with an average of 80 welds per shift. From the results of phases 1 and 2 it is concluded that IWEX imaging technology is available for industrial use and can be regarded as a mature, economical and reliable solution for pipeline cross-sectional inspection [42].

Various studies were conducted in three applications of dementia using aperture focusing techniques without damaging the medium, the overall focus method (TFM) attracted many researchers because of its ability to provide superior image quality. But its use in multimedia is largely limited by the complexity of point counting (POI) calculations and the increasing amount of ultrasonic data obtained. This paper presents a novel 3D-TFM called line-scan conversion (LSC) 3D-TFM for 3D multi-layered media imaging, which uses line segment conversion scanning algorithms to replace traditional ray-detection methods for calculating POIs. Iterative calculations in the ray tracing method are avoided, which can reduce time complexity by one order of magnitude. Simulation experiments show that LSC 3D-TFM accelerates the imaging process 28 times while maintaining similar results [43].

In addition, synthetic focusing applications have also been used in the study of cobalt-chromium alloy specimens produced on cylinder medium containing defects of size and distribution. The specimens were characterized using immersion, concentrated synthetic aperture (SAFT), gradient, and non-linear ultrasound techniques. The results include efficiency, signal to noise ratio, and results comparison between methods and what are believed to be the first determinants of non-linearity (beta) parameters for additives. The results indicate that the manufacture of additives provides a valuable method for generating reference samples, although additional work is required to confirm the shape and morphology of the defect [44].

3D imaging studies using SAFT allow for fast data acquisition and optimized image focusing. The computational burden for 3D imaging is large for each delay voxel for each A-scan obtained should be calculated, e.g. O (N 5) for N3 voxels and N 2 A scans. For reconstruction of large 3D objects in terms of wavelengths, e.g. 100 (100 λ) 3, the calculation of a volume takes several days on the current multicore PC. If 3D speed of sound distribution is used to correct delays, computation time increases. In this work, the flight-based GPU implementation time (TOFI-SAFT) is presented that speeds up the implementation of the previous GPU for SAFT-corrected sound speeds of 7 to 16 min. with only reduced image quality [45].

Ultrasonic susceptibility plays an important role in the examination of heterogeneous materials so theoretical models are crucial for size improvement. Studies on 3D on several effects of weakening factors. The study was carried out using DREAM.3D Software used to produce 10

different quantum ensembles, each containing 50 equations of ore equated with single symmetry of solid crystals, from which the degradation was calculated. Comparisons are then made with the value of the weaknesses derived from classical theories. These theories often underestimate the spatial and sensorial components of microstructures, assume isotropic statistics, and use spatial correlation functions that have certain exponential shapes. The validity of this assumption is examined by computing space statistics to obtain the most common form of bias. The results show Voigt for nickel at 15MHz shows that the longitudinal and horizontal deflections are about one-third and one-quarter of that obtained from the theory, respectively. These differences are due to the relevant spatial correlation function. The results also show little anisotropy in the weakening. Finally, for micro structures with a narrow distribution of grain size and poor texture, the assumption of decoupling proved to be valid [46].

Testing of metal objects containing defects embedded in different sizes is an important application for quality control. Most of these techniques allow detection of defects, but some methods provide sufficient information for the reconstruction of test images in 3D. Studies use a hybrid laser-transducer system that combines laser-generated ultrasound excitation, and the detection of unrelated ultrasonic transducers. This method completely does not allow access to scanned areas in different mediums and defects from different angles / perspectives. This hybrid system can analyse object volume data and allow images to be reconstructed in the form of 3D embedded defects. The research innovations implemented improved signal processing, using 2D apodization window filtering techniques, implemented in conjunction with synthetic aperture focusing algorithms, to eliminate unwanted effects as the side lobe and wide-angle reflections propagate ultrasound waves, resulting in enhanced 3D rendering of image defects. Studies provide qualitative and quantitative volumetric results that yield valuable information on the location and size of defects [47].

As usual, there are also SAFTs used as probes to allow the focus of various measurements with overlap. Studies using heavy metal plate mediums, where the plate is scanned for fast feed by ultrasonic sensors and results on material quality (entry, hole, crack, etc.) are obtained in real time. This application has a high demand for SAFT usage, due to the computational expense commonly used in post-processing. Therefore, specific tuning of the algorithm and compromise on reconstruction quality versus speed is required [48].

In addition to studies improving signal to noise ratio (SNR) and side resolution, phase-imaging algorithm (PCI) algorithms are used in ultrasonic time-lapse detection (TOFD) for heavy-wall welding. The first two stages are performed, delay operation and volume for TOFD-B image opening data are performed by synthetic aperture focusing (SAFT) technique. In the second stage, the aperture data phase is used to establish a phase coherent factor representing the phase propagation for each pixel in the B-SAFT image. Finally, B-SAFT images are dynamically weighted by phase coherent factors. The results show that PCI is able to suppress the structure noise and increase the SNR by amplifying the contribution of phase information. For austenitic welding with a thickness of 78 mm, the average SNR of three drill holes was Φ3 greater than 30 dB, 20 dB higher than the TOFD-B image. In addition, PCI can improve lateral resolution by improving beam aperture directivity. Compared to TOFD-B images, half-width defects in processed images have decreased by more than 70 percent for 48mm CV thickness [49].

References

[1] G. Toullelan, S. Chatillon, R. Raillon, S. Mahaut, S. Lonné, and S. Bannouf, "Results of the 2016 UT modeling benchmark proposed by the French Atomic Energy Commission (CEA) obtained with models implemented in CIVA software," in AIP Conference Proceedings, 2017, doi: 10.1063/1.4974730.

[2] V. Samaitis and L. Mažeika, "Influence of the spatial dimensions of ultrasonic transducers on the frequency spectrum of guided waves," Sensors (Switzerland), 2017, doi: 10.3390/s17081825.

[3] P. Banumathi and P. R. Tamilselvi, "Fabric deconvolution wiener filter and feature extraction regionprops for locating defects," Int. J. Recent Technol. Eng., 2019, doi: 10.35940/ijrte.C5879.098319.

[4] A. B. Lopez, J. Santos, J. P. Sousa, T. G. Santos, and L. Quintino, "Phased Array Ultrasonic Inspection of Metal Additive Manufacturing Parts," J. Nondestruct. Eval., 2019, doi: 10.1007/s10921-019-0600-y.

[5] N. Laroche, E. Carcreff, S. Bourguignon, J. Idier, and A. Duclos, "An Inverse Approach for Ultrasonic Imaging by Total Focusing Point for Close Reflectors Separation," in IEEE International Ultrasonics Symposium, IUS, 2018, doi: 10.1109/ULTSYM.2018.8580073.

[6] E. Maguid, I. Yulevich, D. Veksler, V. Kleiner, M. L. Brongersma, and E. Hasman, "Photonic spin-controlled multifunctional shared-Aperture antenna array," in 2016 IEEE Photonics Conference, IPC 2016, 2017, doi: 10.1109/IPCon.2016.7831039.

[7] R. Hartl, J. Landgraf, J. Spahl, A. Bachmann, and M. F. Zaeh, "Automated visual inspection of friction stir welds: a deep learning approach," 2019, doi: 10.1117/12.2525947.

[8] H. Jin, J. Chen, E. Wu, and K. Yang, "Frequency-domain synthetic aperture focusing for helical ultrasonic imaging," J. Appl. Phys., 2017, doi: 10.1063/1.4979369.

[9] W. Cui and K. Qin, “Fast 3-D Ultrasonic Imaging Using Time-Domain Synthetic Aperture Focusing Techniques Based on Circular Scan Conversions,” IEEE Trans. Comput. Imaging, 2018, doi: 10.1109/tci.2018.2870303.

[10] W. F. Zhu et al., “Time-Domain Topological Energy Imaging Method of Concrete Cavity Defect by Lamb Wave,” Shock Vib., 2019, doi: 10.1155/2019/6294603.

[11] S. Chen, A. Sabato, C. Niezrecki, P. Avitabile, and T. Huber, “Characterization and modeling of the acoustic field generated by a curved ultrasound transducer for non-contact structural excitation,” J. Sound Vib., 2018, doi: 10.1016/j.jsv.2018.06.028.

[12] H. Jin, E. Wu, Y. Han, K. Yang, and J. Chen, “Frequency domain synthetic aperture focusing technique for variable-diameter cylindrical components,” J. Acoust. Soc. Am., 2017, doi: 10.1121/1.5003650.

[13] J. Duan, L. Luo, X. Gao, J. Peng, and J. Li, “Ultrasonic TOFD imaging of weld flaws using wavelet transforms and image registration,” in Proceedings of 2017 IEEE Far East NDT New Technology and Application Forum, FENDT 2017, 2018, doi: 10.1109/FENDT.2017.8584589.

[14] M. Evans, A. Lucas, and I. Ingram, “The inspection of level crossing rails using guided waves,” Constr. Build. Mater., 2018, doi: 10.1016/j.conbuildmat.2018.05.178.

[15] F. Ritter, S. Krempel, S. Tietze, A. Backer, A. Wolfschmitt, and K. S. Drese, “Data transmission by guided acoustic waves,” in Sensoren und Messsysteme - Beitrage der 19. ITG/GMA-Fachtagung, 2020.

[16] N. Amiri, G. H. Farrahi, K. R. Kashyzadeh, and M. Chizari, “Applications of ultrasonic testing and machine learning methods to predict the static & fatigue behavior of spot-welded joints,” J. Manuf. Process., 2020, doi: 10.1016/j.jmapro.2020.01.047.

[17] K. Sawaragi, H. J. Salzburger, G. Hübschen, K. Enami, A. Kirihigashi, and N. Tachibana, “Improvement of SH-wave EMAT phased array inspection by new eight segment probes,” Nucl. Eng. Des., 2000, doi: 10.1016/S0029-5493(99)00276-9.

[18] K. Sudhamayee, “Pipeline monitoring using ultrasonic sensors,” Int. J. Eng. Adv. Technol., 2019, doi: 10.35940/ijeat.F1373.0986S319.

[19] F. Dupont-Marillia, M. Jahazi, S. Lafreniere, and P. Belanger, “Design and optimisation of a phased array transducer for ultrasonic inspection of large forged steel ingots,” NDT E Int., 2019, doi: 10.1016/j.ndteint.2019.02.007.

[20] S. Lin, “Observation of ultrasonic wave propagation in centrifugally cast stainless steel,” in AIP Conference Proceedings, 2019, doi: 10.1063/1.5099740.

[21] A. Decharat, S. Wagle, A. Habib, S. Jacobsen, and F. Melandsø, “High frequency copolymer ultrasonic transducer array of size-effective elements,” Smart Mater. Struct., 2018, doi: 10.1088/1361-665X/aa91b7.

[22] L. Torres, J. Bergman, and M. Fowler, “Ultrasonic NDE technology comparison for measurement of long seam weld anomalies in low frequency electric resistance welded pipe,” in Proceedings of the Biennial International Pipeline Conference, IPC, 2018, doi: 10.1115/IPC201878704.

[23] L. Torres, M. Fowler, and J. Bergman, “Ultrasonic NDE Technology Comparison for Measurement of Long Seam Weld Anomalies in Low Frequency Electric Resistance Welded Pipe,” 2018, doi: 10.1115/ipc2018-78704.

[24] S. W. Glass et al., “Cold spray NDE for porosity and other process anomalies,” in AIP Conference Proceedings, 2018, doi: 10.1063/1.5031507.

[25] M. Clark et al., "Spatially resolved acoustic spectroscopy (SRAS) microstructural imaging," in AIP Conference Proceedings, 2019, doi: 10.1063/1.5099705.

[26] E. Shaswary, J. Tavakkoli, and J. C. Kumaradas, "Efficient Frequency-Domain Synthetic Aperture Focusing Techniques for Imaging with a High-Frequency Single-Element Focused Transducer," IEEE Trans. Ultrason. Ferroelectr. Freq. Control, 2019, doi: 10.1109/TUFFC.2018.2881726.

[27] S. E., T. J., and K. J.C., "Efficient Frequency-Domain Synthetic Aperture Focusing Techniques for Imaging With a High-Frequency Single-Element Focused Transducer," IEEE Trans. Ultrason. Ferroelectr. Freq. Control, 2019, doi: 10.1109/TUFFC.2018.2881726 LK - http://elinks.library.upenn.edu/sfx_local?sid=EMBASE&issn=15258955&id=doi:10.1109%2FTUFFC.2018.2881726&atitle=Efficient+Frequency-Domain+Synthetic+Aperture+Focusing+Techniques+for+Imaging+With+a+High-Frequency+Single-Element+Focused+Transducer&stitle=IEEE+Trans+Ultrason+Ferroelectr+Freq+Control&title=IEEE+transactions+on+ultrasonics%2C+ferroelectrics%2C+and+frequency+control&volume=66&issue=1&spage=57&epage=70&aulast=Shaswary&aufirst=Elyas&auinit=E.&aufull=Shaswa.

[28] M. Spies and H. Rieder, "Enhancement of the POD of flaws in the bulk of highly attenuating structural materials by using SAFT processed ultrasonic inspection data," Mater. Test., vol. 52, no. 3, pp. 160–165, 2010.

[29] Suprijanto, D. Kurniadi, and Sinta, "Modelling and Simulation 3D Ultrasound Wave Propagation using k-space Pseudospectral Method in the Railway Track Geometry," in Proceedings of the 2019 6th International Conference on Instrumentation, Control, and Automation, ICA 2019, 2019, doi: 10.1109/ICA.2019.8916739.

[30] E. G. Bazulin and D. M. Sokolov, "Reconstruction of Ultrasound Reflector Images from Incomplete Data Using the Compressive Sensing Method," Acoust. Phys., 2019, doi: 10.1134/S1063771019040031.

[31] J. Li, Z. Shen, X. Ni, L. Yuan, and C. Ni, "Laser-Ultrasonic Non-Destructive Detection Based on Synthetic Aperture Focusing Technique," Zhongguo Jiguang/Chinese J. Lasers, 2018, doi: 10.3788/CJL201845.0904003.

[32] H. Seo, D. K. Pyun, and K. Y. Jhang, "Synthetic aperture imaging of contact acoustic nonlinearity to visualize the closing interfaces using tone-burst ultrasonic waves," Mech. Syst. Signal Process., 2019, doi: 10.1016/j.ymssp.2018.08.025.

[33] M. Y. Matuda, F. Buiochi, and J. C. Adamowski, "Experimental analysis of surface detection methods for two-medium imaging with a linear ultrasonic array," Ultrasonics, 2019, doi: 10.1016/j.ultras.2018.12.004.

[34] K. Nakahata et al., "Three-dimensional SAFT imaging for anisotropic materials using photoacoustic microscopy," Ultrasonics, 2019, doi: 10.1016/j.ultras.2019.05.006.

[35] D. Ghosh, Rahul, A. Ganguli, and A. Mukherjee, "Ultrasonic imaging as a diagnostic tool for detection of rebar corrosion," in Proceedings of the 7th Asia-Pacific Workshop on Structural Health Monitoring, APWSHM 2018, 2018.

[36] I. Petrov, A. Vdovenko, D. Dolmatov, and D. Sednev, "The implementation of post-processing algorithm for ultrasonic testing of welds," in IOP Conference Series: Materials Science and Engineering, 2019, doi: 10.1088/1757-899X/510/1/012004.

[37] J. Vrana, K. Schörner, H. Mooshofer, K. Kolk, A. Zimmer, and K. Fendt, "Ultrasonic Computed Tomography − Pushing the Boundaries of the Ultrasonic Inspection of Forgings," Steel Res. Int., 2018, doi: 10.1002/srin.201700448.

[38] J. Tarraf et al., "Application of ultrasonic waves towards the inspection of similar and dissimilar friction stir welded joints," J. Mater. Process. Technol., 2018, doi: 10.1016/j.jmatprotec.2018.01.006.

[39] D. Lévesque et al., "Inspection of thick welded joints using laser-ultrasonic SAFT," Ultrasonics, 2016, doi: 10.1016/j.ultras.2016.04.001.

[40] C. W. Tseng, Y. F. Chang, and C. Y. Wang, "Total focusing method or phased array technique: Which detection technique is better for the ultrasonic nondestructive testing of concrete?," J. Mater. Civ. Eng., 2018, doi: 10.1061/(ASCE)MT.1943-5533.0002118.

[41] J. Brizuela, J. Camacho, G. Cosarinsky, J. M. Iriarte, and J. F. Cruza, "Improving elevation resolution in phased-array inspections for NDT," NDT E Int., 2019, doi: 10.1016/j.ndteint.2018.09.002.

[42] J. Van Der Ent, A. Fandika, G. Brisac, L. Pinier, and L. Pomie, "Validation and qualification of IWEX 3D ultrasonic imaging for girth weld inspection," in Rio Pipeline Conference and Exposition, Technical Papers, 2017.

[43] W. Cui and K. Qin, "Real-Time Total Focusing Method Imaging for Ultrasonic Inspection of Three-Dimensional Multilayered Media," in ICASSP, IEEE International Conference on Acoustics, Speech and Signal Processing - Proceedings, 2018, doi: 10.1109/ICASSP.2018.8462130.

[44] L. Koester et al., "NDE of additively manufactured components with embedded defects (reference standards) using conventional and advanced ultrasonic methods," in AIP Conference Proceedings, 2017, doi: 10.1063/1.4974721.

[45] N. V. Ruiter, E. Kretzek, M. Zapf, T. Hopp, and H. Gemmeke, "Time of flight interpolated synthetic aperture focusing technique," in Medical Imaging 2017: Ultrasonic Imaging and Tomography, 2017, doi: 10.1117/12.2254259.

[46] M. Norouzian and J. A. Turner, "Ultrasonic wave propagation predictions for polycrystalline materials using three-dimensional synthetic microstructures: Attenuation," J. Acoust. Soc. Am., 2019, doi: 10.1121/1.5096651.

[47] H. Selim, J. Trull, M. D. Prieto, R. Picó, L. Romeral, and C. Cojocaru, "Fully noncontact hybrid NDT for 3D defect reconstruction using SAFT algorithm and 2D apodization window," Sensors (Switzerland), 2019, doi: 10.3390/s19092138.

[48] F. Krieg, J. Kirchhof, F. Romer, A. Ihlow, G. Del Galdo, and A. Osman, "Implementation issues of 3D SAFT in time and frequency domain for the fast inspection of heavy plates," in IEEE International Ultrasonics Symposium, IUS, 2017, doi: 10.1109/ULTSYM.2017.8091971.

[49] Y. Chen et al., "Research on Ultrasonic TOFD Imaging Inspection for Heavy-walled Weld Based on Phase Coherence Characteristics," Jixie Gongcheng Xuebao/Journal Mech. Eng., 2019, doi: 10.3901/JME.2019.04.025.